Journal of the American Heart Association

ORIGINAL RESEARCH

Stressor-Evoked Brain Activity, Cardiovascular Reactivity, and Subclinical Atherosclerosis in Midlife Adults

Javier Rasero, PhD; Timohy D. Verstynen, PhD; Caitlin M. DuPont, PhD; Thomas E. Kraynak, PhD; Emma Barinas-Mitchell, PhD; Mark R. Scudder, PhD; Thomas W. Kamarck, PhD; Amy I. Sentis, PhD; Regina L. Leckie, PhD; Peter J. Gianaros, PhD

BACKGROUND: Cardiovascular responses to psychological stressors have been separately associated with preclinical atherosclerosis and hemodynamic brain activity patterns across different studies and cohorts; however, what has not been established is whether cardiovascular stress responses reliably link indicators of stressor-evoked brain activity and preclinical atherosclerosis that have been measured in the same individuals. Accordingly, the present study used cross-validation and predictive modeling to test for the first time whether stressor-evoked systolic blood pressure responses statistically mediated the association between concurrently measured brain activity and a vascular marker of preclinical atherosclerosis in the carotid arteries.

METHODS AND RESULTS: Six hundred twenty-four midlife adults (aged 28–56 years, 54.97% women) from 2 different cohorts underwent 2 information-conflict functional magnetic resonance imaging tasks, with concurrent systolic blood pressure measures collected. Carotid artery intima-media thickness was measured by ultrasonography. A mediation framework that included harmonization, cross-validation, and penalized principal component regression was then used. Brain areas where functional magnetic resonance imaging activity exhibited reliable direct and indirect effects were identified through bootstrapping. Sensitivity analysis further tested the robustness of findings after accounting for prevailing levels of cardiovascular disease risk and brain imaging data quality. Task-averaged patterns of functional magnetic resonance imaging activity across distributed brain areas exhibited a generalizable association with carotid artery intima-media thickness, which was reliably mediated by an area under the curve measure of aggregate systolic blood pressure reactivity. Importantly, this effect held in sensitivity analyses. Implicated brain areas in this mediation included the ventromedial prefrontal cortex, anterior cingulate cortex, insula, and amygdala.

CONCLUSIONS: These novel findings support a link between stressor-evoked brain activity and preclinical atherosclerosis, which is accounted for by individual differences in corresponding levels of stressor-evoked cardiovascular reactivity.

Key Words: cardiovascular reactivity ■ carotid artery intima-media thickness ■ functional magnetic resonance imaging ■ mediation ■ psychological stress

Acute psychological stressors, defined in a stress typology framework[1,2] as short-term demands that are appraised as taxing or exceeding one's coping resources,[3] typically raise blood pressure (BP) and alter other parameters of cardiovascular physiology in most people.[4–7] There are wide and stable

Correspondence to: Peter J. Gianaros, PhD, Department of Psychology, University of Pittsburgh, 3131 Sennott Square, 210 S. Bouquet Street, Pittsburgh, PA 15260. Email: gianaros@pitt.edu and Javier Rasero, PhD, School of Data Science, University of Virginia, PO Box 400249, Charlottesville, VA 22904, Email: jrasero.daparte@gmail.com

This article was sent to Jose R. Romero, MD, Associate Editor, for review by expert referees, editorial decision, and final disposition.

Preprint posted on MedRxiv February 06, 2024. doi: https://doi.org/10.1101/2024.02.05.24302236.

Supplemental Material is available at https://www.ahajournals.org/doi/suppl/10.1161/JAHA.124.034908

For Sources of Funding and Disclosures, see page 15.

JAHA is available at: www.ahajournals.org/journal/jaha

CLINICAL PERSPECTIVE

What Is New?

- Using neuroimaging, blood pressure monitoring, mental stress testing, and machine-learning methods in midlife adults, brain patterns were identified that predicted subclinical atherosclerosis.
- The links between brain patterns and subclinical atherosclerosis were explained by stress-related blood pressure.

What Are the Clinical Implications?

- Mental stress contributes to risk for cardiovascular disease. Neuroimaging may aid in identifying and intervening on the brain–body pathways that contribute to this stress-related risk.

Nonstandard Abbreviations and Acronyms

MSIT	multisource interference task
NOAH	Neurobiology of Adult Health
PIP	Pittsburgh Imaging Project

(phenotypic) differences across people, however, in the magnitude, patterning, duration, and direction of stressor-evoked cardiovascular, particularly BP, reactions.[8] According to several conceptual frameworks on psychological stress, BP reactions to acute stressors arise from predictive processes that are instantiated in brain systems for visceral control, which are thought to adjust cardiovascular physiology to meet the anticipated metabolic demands that are necessary to cope with acute stressors.[9–12] Notably, some people have a trait-like phenotype to exhibit larger than average rises in BP that may exceed the metabolic demands of a stressor.[9] When assessed by standard stressor batteries and testing paradigms, the magnitude of stressor-evoked BP reactions generalizes from the laboratory to predict those measured in daily life via ambulatory BP monitoring.[8,13] The latter evidence has been interpreted to support the possibility that a phenotype to repeatedly express large-magnitude stressor-evoked BP reactions over the life course may confer cardiovascular risk via their cumulative pathophysiological effects on the vasculature.

In the context of cardiovascular health, for example, epidemiological evidence demonstrates that greater stressor-evoked BP reactivity predicts vascular pathology[14,15] and early death,[16] consistent with the interpretation that large BP reactions to acute stressors may eventuate in vascular risk, reflected by arterial changes and dysfunction.[17–24] These pathogenic effects may result from repeated pressor influences that injure the endothelial layer of blood vessels via turbulent (nonlaminar) blood flow and shear stress.[6,25] At the vascular level, such injury may increase the permeability of the endothelium to lipoproteins, promote the release of mitogenic substances, contribute to the proliferation of intimal smooth muscle cells, and disrupt the lipid metabolism of endothelial cells.[26–28] The effects of a phenotype to exhibit large-magnitude stressor-evoked BP reactivity may thus manifest as endothelial damage and dysfunction, as well as a hypertrophy or thickening of arteries and other blood vessels.[6,29] Consistent with these interpretations, exaggerated stressor-evoked BP reactivity predicts end points of the latter pathological changes, including hypertension and a surrogate marker of preclinical vascular disease, namely, carotid artery thickening.[16,30,31]

In parallel to the latter epidemiological findings on preclinical vascular disease, human brain imaging studies have identified functional patterns of neural activity that predict individual differences in stressor-evoked BP reactivity, particularly patterns that have been localized to what have been termed visceral control circuits.[9]

Visceral control circuits encompass evolutionarily conserved networks of brain areas spanning the medial prefrontal cortex, anterior cingulate, insula, hippocampus, amygdala, thalamus, hypothalamus, periaqueductal gray, and brainstem cell groups. These circuits control and coordinate autonomic, neuroendocrine, hemodynamic, and immune activity across a range of behavioral states that affect cardiovascular physiology and pathophysiology, especially in relation to stressful and emotional experiences that may confer cardiovascular risk. In these regards, visceral control circuits are brain systems that may orchestrate psychological appraisal processes of stressors that are calibrated with peripheral physiology to support adaptive action and stressor coping behaviors. Accordingly, visceral control circuits are hypothesized to be capable of mechanistically orchestrating behavioral influences on cardiovascular risk via several peripheral physiological mechanisms,[6,32] including central neural control over peripheral autonomic and neuroendocrine determinants of acute stressor-evoked BP reactivity.[9] For example, preclinical animal evidence indicates that visceral control circuits are capable of gating or modifying the baroreflex, which may proximally contribute to the magnitude of stressor-evoked rises in BP.[9]

What has not yet been firmly established, however, is the extent to which stressor-evoked BP reactivity per se statistically explains the possible association of functional activity within visceral control circuits and established subclinical markers of cardiovascular risk, particularly carotid artery thickening. Therefore,

the present study used a predictive machine-learning approach to test the hypothesis that multivariate features of stressor-evoked activity within visceral control circuits of the brain are associated with carotid artery thickening in part via stressor-evoked BP reactivity within a statistical mediation model. Participants from 2 cohort studies of the neural correlates of stress physiology and cardiovascular risk (total n=624 midlife adults; aged 28–56 years [54.97% women]) completed a battery of psychological stress tasks designed to measure reliable individual differences (phenotypes) in self-reported and cardiovascular reactivity to acute stressors while hemodynamic responses in the brain were monitored using functional magnetic resonance imaging (fMRI).[33–36] For completeness of reporting, prediction models tested a range of different measures of cardiovascular stress reactivity and physiology.

METHODS

Participants

Cross-sectional data used herein were from midlife and community-dwelling adults who participated in 2 different studies with harmonized data collection protocols. The first was the Pittsburgh Imaging Project (PIP), which included 325 individuals (aged 30–51 years, 163 women and 162 men, 226 identifying as White,79 identifying as Black, 15 identifying as Asian, 3 identifying as multiracial, and 2 reporting other racial identities). In the PIP cohort, 79.26% reported never having smoked, 16.06% reported being former smokers, and 4.68% reported being current smokers. The second cohort was comprised of participants in the Neurobiology of Adult Health (NOAH) study, which included 299 individuals (aged 28–56 years, 180 women and 110 men, 1 identifying as neither woman nor man, 254 identifying as White, 18 identifying as Black, 19 identifying as Asian, 7 identifying as multiracial, and 1 reporting as another racial identity). In the NOAH cohort, 63.08% reported never having smoked, 20% reported being former smokers, and 16.92% reported being current smokers. Informed consent was obtained from all participants, and approval was granted by the University of Pittsburgh Human Research Protection Office for PIP (protocol ID: 07110287) and NOAH (19030012).

Recruitment methods and related methodological details for the PIP cohort have been published.[34,37] Exclusionary criteria for the PIP cohort included: aged <30 or >50 years; metallic or other implants unsafe for MRI; pregnancy; any self-reported history of cardiovascular disease (CVD); any self-reported history of a neurological disorder; current treatment for or self-reported diagnoses by a health care professional of a psychiatric condition; consuming alcohol equaling or exceeding 5 servings ≥3 times/week; regular use of over-the-counter or prescribed medications with autonomic, cardiovascular, or neuroendocrine effects, including daily use of corticosteroid inhalers; any current treatment for hypertension or having a resting BP exceeding 140/90 mm Hg; use of any psychotropic medications (eg, antidepressants); history of metal exposure (eg, welding); and color blindness.

Recruitment methods for the NOAH cohort involved (1) mass electronic and print mailings to residents of Allegheny County, Pennsylvania; (2) radio, electronic (eg, Craigslist), and print advertisements in public places (eg, Port Authority Buses, local newspapers, community and park announcement boards); and (3) direct solicitation from the participant registries of the University of Pittsburgh's Clinical and Translational Science Institute Pitt+Me Registry and University Center for Social and Urban Research Regional Research Registry. Exclusionary criteria for the NOAH cohort included: aged <28 or >56 years; self-reported use of medications with central or peripheral autonomic effects on ≥1 occasion in the 14 days before testing (including antihypertensive or cardiac medications, antipsychotic medications, protease inhibitors or other anti-HIV medications, insulin, chemotherapy agents, immunosuppressants, prescription weight-loss medications, and ephedrine); regular use (ie, use on ≥7 days in the 14 days before testing) of antianxiety medications, sleep medications, asthma medications and allergy inhalants, antidepressant medications, glucocorticoids, medical marijuana, more than 2 non-insulin medications for diabetes; consuming ≥35 alcoholic drinks in the past 7 days; consuming ≥6 alcoholic drinks on ≥3 occasions in the past 7 days; use of illicit drugs on ≥7 days in the past 2 weeks; major medical conditions, including CVD, severe hypertension (systolic blood pressure [SBP]>160 or diastolic blood pressure [DBP] >100 mm Hg); cancer (treatment in past 12 months, except for nonmelanoma skin cancer), liver disease, chronic kidney disease, and type 1diabetes; self-reported history of a major neurological disorder or brain injury resulting in ongoing symptoms or cognitive impairment (eg, multiple sclerosis, cerebral palsy, major head injury); history of schizophrenia or bipolar disorder; lung disease requiring regular or ongoing drug treatment; weight loss surgery within the past 5 years; for women, pregnancy; regular use of an assistive walking device; nonfluency in English; visual impairments affecting comprehension of printed text or text on a computer screen; color blindness; contraindications for magnetic resonance imaging; night shift employment on a frequent basis (operationally defined as working half or more of employment hours in a full workday between midnight and 8 AM, and this occurring >12 times during the past year); and lack of reliable access to a telephone throughout the day (home, work, or cell phone).

Cardiovascular Risk Factors

At the time of initial testing, participants in both studies underwent assessments of seated resting blood pressure, waist circumference, and body mass index, as well as fasting glucose and lipid levels. Following guidelines of the American Heart Association, seated resting blood pressures (BPs) were obtained with an oscillometric device (PIP: Critikon Dinamap 8100, Johnson & Johnson, Tampa, FL; NOAH: Omron IntelliSense BP Monitor, model HEM-907XL, Omron Healthcare). A total of 3 BPs were taken after an acclimation period, with the average of the last 2 of the 3 BPs being used to compute resting SBP and DBP. Participants' waist circumference was measured at the level of the umbilicus to the nearest half centimeter at end expiration. Height was measured by a vertical-mounted stadiometer (with shoes off), and weight was measured in kilograms.

Similarly, at the time of initial testing, participants underwent fasting phlebotomy for the assessment of glucose, insulin, total cholesterol, triglycerides, and high-density lipoprotein cholesterol. If participants were unable to comply with prephlebotomy instructions, they were rescheduled. Along with other demographic and anthropometric variables, these measures were used to describe and characterize the study sample and to derive the 10-year atherosclerotic cardiovascular disease (ASCVD) risk score.[38] To this end, the following variables were entered into the Cardiovascular Risk computational package (version 1.1.1; https://github.com/vcastro/CVrisk), which was implemented in R statistical software[39]: age, sex at birth, race, cholesterol, high-density lipoproteins, SBP, smoking status, use of BP-lowering medication, and diabetes status. In the present study and in line with the preregistered analysis plan, race was used in the calculation of 10-year ASCVD risk scores per its formulation by Goff et al[40]; however, race was construed herein as a social construct and included to account for the potential influence of inequalities in exposures to systemic racism and discrimination, as well as inequalities in access to opportunities among those who do not identify as White.[41,42] Additional 10-year ASCVD risk scores that include only age, sex at birth, cholesterol, high-density lipoproteins, SBP, smoking status, and diabetes status per the earlier formulation of D'agostino et al[43] are publicly accessible for the present participants (see Preregistration and Availability of Code and Data below).

Carotid Artery Intima-Media Thickness by Ultrasonography

Participants in both cohorts underwent the same carotid artery ultrasonography protocol, which was performed by a registered vascular technologist in the laboratory of coauthor E.B.-M. Specifically, each participant laid supine with the head tilted at 45°, and, using an Acuson Antares scanner (Acuson-Siemens, Malvern, PA), the technologist performed scout views of the left and right carotid arteries in both the transverse and longitudinal planes. A region-of-interest encompassing the artery walls was identified for more focused B-mode imaging of 3 carotid areas: (1) the near and far walls of the distal common carotid artery (1 cm proximal to the carotid bulb, measured in duplicate on each side and averaged across images and sides); (2) the far wall of the carotid bulb (defined as the point where the near and far walls of the common carotid are no longer parallel and extending to the flow divider); and (3) the first centimeter of the internal carotid (defined distally from the edge of the flow divider). For the 3 carotid areas (common, bulb, and internal), an optimal image was digitized for later scoring with automated edge detection software (Artery Measurement System; Goteborg University, Gothenburg, Sweden). The software was used to draw 2 lines: 1 along the lumen–intima interface and 1 along the media–adventitia interface. The distances between the line-identified interfaces were measured in 1 cm segments, generating 1 measurement (in millimeters) for each pixel in each segment (approximately 140 measurements total). As preregistered, the primary dependent (Y) variable in the present analyses corresponded to the mean average carotid artery intima media thickness (CA-IMT) averaged over the far walls of the carotid bulb and common carotid artery.

fMRI Stressor Task Battery

The tasks of this battery include a Stroop task and a multisource interference task (MSIT), each 9 minutes 20 seconds. Both entail processing conflictual information, receiving negative feedback, and making time-pressured responses to unpredictable and uncontrollable stimuli that elicit subjective distress.[36] Briefly, subjects complete 4, 52- to 60-second blocks of trials in both tasks that define a congruent condition, which are interleaved with 4, 52- to 60-second blocks of trials defining an incongruent condition. Conditions are preceded by a 10- to 17-second fixation period. In the Stroop, subjects identify the color of target words in the center of a screen by selecting 1 of 4 identifier words. Selections are made by pressing 1 of 4 buttons on a glove, with each button matching an identifier word on the screen (eg, thumb button 1=identifier word on the left). During congruent Stroop trials: (1) targets are in colors congruent with the target words, and (2) identifiers are in the same colors as targets. During incongruent Stroop trials: (1) targets are in colors incongruent with the targets, and (2) identifiers are in colors incongruent with the colors that the

identifiers name. In the MSIT, subjects in the NOAH study selected a number that differed from 4 others by pressing 1 of 4 buttons on the glove, with each button matching a number on the screen (thumb button 1=number 1). During congruent MSIT trials, targets were in a position compatible with their position on the glove. During incongruent MSIT trials, targets were in a position incompatible with their glove position. In the PIP study, subjects were presented with 3-number stimuli and not 4 as in NOAH. One methodological difference is that although the PIP study used 0s in the MSIT to indicate an incompatible position in the congruent condition (eg, 1 0 0), NOAH used 1 number between 1 and 4 (eg, 1 2 2 2) during this condition. In incongruent conditions of both tasks in both cohorts, accuracy was held to ≈50% by adjusting intertrial intervals. Thus, consecutive accurate performance in an incongruent condition prompted shorter intertrial intervals. Conversely, less accurate performance lengthened intertrial intervals. To control for motor response differences between conditions, the number of trials in the congruent condition was yoked to the number completed in the incongruent condition. To implement yoking, (1) an incongruent block is administered first, and (2) congruent condition trials appear at the mean intertrial interval of the preceding incongruent block.

Cardiovascular Reactivity

During fMRI testing, BP was measured using magnetic resonance imaging-compatible devices (PIP: Medrad Multigas 9500, Warrendale, PA/Leverkusen, Germany; NOAH: Tesla M3 Magnetic Resonance Imaging Patient Monitor by the Mammendorf Institute for Physiology and Medicine, Mammendorf, Germany). The average incongruent condition–minus–average baseline BP=difference was used to compute reactivity. Systolic SBP reactivity values, or ΔSBP, averaged across tasks to keep an analytical procedure comparable to that with activation patterns (see following subsections), were used as the primary mediator variable (M) in our study. In addition, we have previously shown that task-averaged reactivity scores from this stressor battery exhibit higher levels of test–retest reliability than those from individual tasks.[36] Further analyses that were preregistered also considered other reactivity metrics, including (1) the area under the curve with respect to ground, or SBP_AUC$_g$; and (2) the area under the curve with respect to increase,[44–46] or SBP_AUC$_i$, conditional on these alternative metrics of reactivity exhibiting statistical associations with CA-IMT. The area was calculated for the curve formed by the baseline SBP measure, defined as the average of the last 2 SBP values taken inside the scanner before the onset of the tasks, and subsequent average SBP values for each condition (incongruent or congruent), following the order of the task sequence (see Figure S1, and Figure S2 for DBP). For SBP_AUC$_g$, the coordinate origin was set at 0, whereas for SBP_AUC$_i$, it was set at the baseline. Unlike ΔSBP, both area under the curve measures incorporate SBP changes throughout the entire task. As a result, they are capable of capturing more information, such as subject habituation to the task and the total or aggregate load of BP throughout the entire task as opposed to the average peak increase. Moreover, area under the curve measures have been shown to exhibit better phenotypic test–retest reliability compared with measures like ΔSBP.[47]

Magnetic Resonance Imaging Data Acquisition and Preprocessing

Imaging in the PIP cohort was conducted using a 3T Trio TIM scanner (Siemens, Erlangen, Germany). Functional blood oxygen level dependent (BOLD) data for the Stroop and MSIT tasks were acquired with a gradient echo-planar imaging sequence by these parameters: time to repetition/time to echo=2000/28 ms; matrix resolution=64×64; field of view=205×250 mm; and flip angle=90°. Each volume was 3 mm in thickness, with no gap (280 task volumes in total, excluding 4 discarded volumes). Before functional imaging, a T1-weighted magnetization prepared rapid gradient echo structural image was obtained by these parameters: repetition time=2100 ms; inversion time=1100 ms; echo time=3.31 ms; flip angle=8°. There were 192 sagittal slices (1-mm thick, no spaces between slices) having a matrix size of 256×208 pixels (field of view=256×208 mm).

In the NOAH study, imaging was conducted using a 3T PRISMA scanner (Siemens), which was equipped with a 64-channel head coil. Before functional imaging, a T1-weighted magnetization prepared rapid gradient echo structural image was obtained by these parameters: repetition time=2300 ms; inversion time=900 ms; echo time=1.99 ms; flip angle=9°. There were 176 sagittal slices (1-mm thick, no spaces between slices) having a matrix size=176×176 voxels (field of view=256×256 mm). Functional BOLD image acquisition parameters for the Stroop and MSIT tasks were: matrix size=106×106 voxels (field of view=212×212 mm), repetition time=2000 ms, echo time=30 ms, and flip angle=79°. Sixty-nine slices per volume were collected along an anterior-to-posterior encoding direction. Each volume was 2 mm in thickness, with no gap (280 task volumes in total, excluding 4 discarded volumes).

Individual fMRI data for both cohorts and tasks underwent the same preprocessing pipeline using statistical parametric mapping software (SPM12; http://www.fil.ion.ucl.ac.uk/spm). For spatial preprocessing, T1-weighted magnetization prepared rapid gradient echo images were classified into 6 tissue types.

Biased-corrected and deformation field maps were then computed. Functional images were realigned to the first image of the series by a 6-parameter rigid-body transformation, using the reslice step to match the first image on a voxel-by-voxel basis. Before realignment, slice-timing correction was applied to account for acquisition time variation. Realigned images were coregistered to each participant's skull-stripped and biased-corrected magnetization prepared rapid gradient echo image. Coregistered images were normalized to Montreal Neurological Institute space. In within-individual fMRI analyses, univariate general linear models were estimated to compute contrast maps used for prediction and mediation analysis described below in the analysis plan. Task blocks were modeled by rectangular waveforms convolved with the default hemodynamic response function in SPM12. These regressors modeled blocks (ie, fixation, incongruent condition, congruent condition). In each general linear model, the 6 realignment parameters from preprocessing were included as nuisance regressors, and low-frequency artifacts were removed by a high-pass filter (187 seconds). To further remove artifact effects from fMRI data while keeping all time points, error variance was estimated and then weighted by restricted maximum likelihood estimation, as implemented in the RobustWLS toolbox version 4.0. In this approach, time points were inversely weighted according to the residual noise over the whole brain, so volumes with larger levels of residual noise had less contribution to the first-level estimations. Subsequently, each estimated task condition parameter was smoothed by a 6-mm full width at half maximum Gaussian kernel. Linear contrasts, computed as incongruent versus congruent condition effects and averaged across Stroop tasks and MSIT, constituted the independent variable (X) in our main analysis (see next section). This step of averaging across both tasks was performed to maintain comparability with prior work,[34] as well as to reduce measurement error and increase reliability as previously demonstrated for this stressor battery.[36]

Exclusion criteria of individual fMRI data included lack of spatial (brain) coverage, incomplete sequence acquisition, experimental error, equipment malfunction during participant testing, and lack of participant task comprehension after reviewing task performance and experimenter notes.

Statistical Analysis

A mediation framework was used to test the association between the task-averaged whole-brain fMRI incongruent versus congruent activity maps (the multivariate independent variable, X) and CA-IMT (the univariate outcome variable, Y), mediated by task-averaged in-scanner SBP reactivity (the univariate mediator, M). To accomplish this and following Baron and Kenny's steps,[48] the X-to-Y (total effect) or *c* path was first assessed, that is, the relation between the task-averaged stressor-evoked fMRI activation patterns and the CA-IMT. Next, the X-to-M or *a* path was estimated, that is, the effect of the task-averaged stressor-evoked fMRI activation patterns on task-averaged stressor-evoked SBP reactivity. Finally, the *b* and *c′* paths were estimated, which are defined as the amount of variability of Y that M and X respectively explain when taken together in the same model ([X+M]-to-Y). As a result, statistical evidence for a *c′* path indicates that X has a direct effect on Y. Similarly, statistical evidence for both *a* and *b* paths indicates that X has an effect on Y mediated by M (indirect effect). To note, the whole mediation scenario was conducted separately for each potential mediator (ΔSBP, SBP_AUC_g, and SBP_AUC_i).

In the current modeling framework, the aforementioned mediation scenario was tested using a multivariate machine-learning approach, which typically outperforms univariate efforts by exhibiting a better ability to map complex associations, and a better test–retest reliability and internal consistency.[49] Specifically, in each mediation step, a typical approach[37,50–52] that uses a principal component analysis followed by penalized regression was adopted. A principal component analysis was used to address the high degree of dimensionality of our input data (ie., number of features much greater than the number of observations) and to account for the high degree of collinearity across voxels (exacerbated by spatial smoothing). Penalized regression was then used to find the most parsimonious version of the model possible. In our study, both L1 (also known as Lasso) and L2 (also known as Ridge) penalization techniques were separately tested. The exact form of these penalization terms, along with the quantitative steps involved in our predictive approach, are detailed in Data S1.

Following recommendations for best practice in prediction studies,[53] the reliability of each effect was assessed using a nested k-fold cross-validation, consisting of (1) an inner loop 5-fold cross-validation to optimize the predictive models, and (2) an outer loop 10-fold cross-validation to determine the predictive generalizability of these models. This data splitting took place separately in each mediation analysis conducted and in a stratified fashion, so M and Y variables did not differ statistically between training and test sets. Stratification also took cohort information into account, ensuring that both studies were included during training and testing while maintaining the original proportion between them. The whole cross-validation procedure was also repeated with 5 different seeds to account for the variability when splitting the data.

The generalizability of each optimal predictive model (ie, X-to-Y, X-to-M and [X+M]-to-Y models) was evaluated by comparing predicted with observed

outcome variables in the test samples. Here, the similarity between predicted and observed values was summarized by Pearson correlation coefficients and corresponding 95% bootstrapped CIs and *P* values. Following guidelines for predictive modeling,[53] variance in observed values explained by predicted values (R^2) was calculated by the sums-of-squares formulation. Furthermore, to estimate the generalizability of the mediation effect the following measure was adopted: $R^2_{med} = R^2_{M\to Y} - \left(R^2_{X+M\to Y} - R^2_{X\to Y}\right)$. This is based on the effect sizes of each individual model in the mediation analysis framework[54] and therefore easily evaluated out-of-sample. Finally, the evidence for each effect was quantified using Bayes factors, BF_{10}, which reflect the ratio between the probability of the alternative (existence of a positive correlation between predicted and observed values) and the null hypotheses (absence of or negative correlation between predicted and observed values).

Individual features that reliably contributed to both direct effects (or *c′* path) and indirect effects (ie, the products *a*×*b*) were determined by bootstrap resampling (5000 resamples), with corrections for a false discovery rate of 0.05.[55] This analysis was performed on the principal component space to increase statistical power and included a transformation to encoding models to ensure a correct interpretation of the resulting weight maps.[56] The details of this bootstrapping procedure can be found in Data S1.

Importantly, because of the use of 2 different cohorts, harmonization techniques were applied with the aim of reducing the differences between NOAH and PIP. In particular, for neuroimaging data (X), ComBat was adopted, which is a Bayesian-based statistical method that has been shown to adjust for location and scale effects from different data sources.[57] M and Y were similarly harmonized by standardizing them within cohorts.

Finally, it is important to note that each of the different steps that led to the final predictions (harmonization, dimensionality reduction) were all part of the analytical pipeline and, more importantly, were embedded within the cross-validation procedure, thus preventing any data leakage.

Ancillary Analysis

One fundamental difficulty in any mediation analysis is the violation of the sequential ignorability assumptions due to the existence of unobserved confounders causally affecting both the mediator and the outcome even after conditioning on the observed levels of the input (treatment variable) and pretreatment covariates.[58] For example, observed changes in cardiovascular reactivity and preclinical atherosclerosis from neural responses to stress could be explained by prevailing levels of overall CVD risk of each individual in our study. To address this possibility, the 10-year ASCVD risk scores were used as control variables to examine the influence on predicted versus observed correlation values. This analysis was contingent on the existence of a significant correlation between ASCVD risk scores and CA-IMT, and for any of the cardiovascular reactivity measures tested where such a significant correlation also existed. Additionally, sensitivity analyses assessed the influence of functional brain imaging data quality by excluding subjects with excessive head motion during any of the task acquisitions (average framewise displacement >0.5 mm using the formula in Power et al[59]). Last, in a deviation from the preregistered analytic plan, metrics of DBP reactivity were explored for an overall comparison to SBP reactivity findings (Data S1).

Preregistration and Availability of Code and Data

Hypotheses and planned analyses were preregistered at Open Science Framework (OSF) on June 1, 2022 (https://osf.io/j278q). Source files and analysis scripts are available at GitHub (https://github.com/CoAxLab/sbp-imt-mediation). Data files, which include the activation patterns, mediator, outcome and confounder variables, along with the fitted predictive models, component loadings and false discovery rate-corrected *P* values, can be found at Figshare (https://figshare.com/s/4e1feb883c9ca6ae7634). Other data may be made available upon reasonable request via a University of Pittsburgh Data Use Agreement. To the authors' awareness, this is the first study to investigate the cross-sectional association between stressor-evoked brain activity patterns and CA-IMT mediated by changes in BP.

RESULTS

Sample Characteristics

Descriptive information for demographic and cardiovascular measures are summarized in Table 1. To note, using Cohen's *d* and the log variability ratio (*lnVR*), statistical differences in the mean and standard deviation of PIP relative to NOAH were observed for the variables entering the mediation model, that is, CA-IMT (*d*=0.36 [95% CI, 0.19–0.54]; *lnVR*=−0.20 [95% CI −0.37 to −0.04]), ΔSBP (*d*=0.22 [95% CI, 0.06–0.37]; *lnVR*=−0.16 [95% CI −0.32 to −0.01]), SBP_AUC_g (*d*=0.65 [95% CI, 0.48–0.82]; *lnVR*=−0.17 [95% CI, −0.29 to −0.04]), SBP_AUC_i (*d*=0.24, [95% CI, 0.08–0.40]; *lnVR*=−0.19 [95% CI, −0.35 to −0.03]), as well as for our control variable, the ASCVD risk score (*d*=0.24

Table 1. Data Characteristics and Descriptive Statistics for the Continuous Variables in the Study

Characteristic	PIP (N=325, 163 women)		NOAH (N=299, 180 women)	
	Mean [95% CI]	SD	Mean [95% CI]	SD
Age, y	40.89 [40.21–41.60]	±6.24	42.31 [41.24–43.6]	±8.64
No. of school y completed	16.67 [16.33–17.04]	±3.31	17.63 [17.32–17.96]	±2.85
Weight, lb	174.13 [170.31–177.98]	±35.44	168.03 [164.26–172.29]	±37.99
Waist, in	38.04 [34.95–43.68]	±47.66	36.81 [36.16–37.43]	±5.56
Height, in	67.46 [67.04–67.88]	±3.71	66.84 [66.42–67.24]	±3.66
Glucose, mg/dL	88.15 [86.91–89.36]	±11.58	87.33 [86.40–88.34]	±8.51
Triglyceride, mg/dL	94.05 [87.68–100.75]	±57.46	97.88 [88.88–110.34]	±89.89
HDL, mg/dL	50.89 [49.16–52.72]	±16.17	57.74 [56.05–59.53]	±14.88
Insulin, μU/mL	8.92 [8.06–9.81]	±6.50	6.72 [6.04–7.38]	±6.01
BMI, kg/m^2	26.88 [26.38–27.42]	±5.08	26.27 [25.59–26.87]	±5.35
CA-IMT, mm	0.64 [0.63–0.65]	±0.10	0.60 [0.59–0.62]	±0.13
Clinic SBP, mm Hg	121.01 [119.76–122.13]	±10.66	114.49 [112.85–116.05]	±13.49
ΔSBP, mm Hg	4.22 [3.57–4.83]	±5.75	2.84 [2.04–3.68]	±6.78
SBP_AUC$_g$, mm Hg/s	1014.78 [1003.33–1025.46]	±100.20	943.60 [929.78–958.16]	±118.43
SBP_AUC$_i$, mm Hg/s	27.85 [23.72–32.45]	±39.13	17.35 [11.60–23.38]	±47.41
ASCVD 10 y	1.90 [1.74–2.11]	±1.69	1.55 [1.42–1.69]	±1.20

Average coefficient of determination, R^2, and 95% CI for each mediator variable (columns) and model path (rows). The mediation effect was calculated using the R^2 values in each path as explained in the Methods section. ASCVD indicates atherosclerotic cardiovascular disease; AUC$_g$, area under the curve with respect to ground; AUC$_i$, area under the curve with respect to increase; BMI, body mass index, CA-IMT, carotid artery intima-media thickness; HDL, high-density lipoprotein; NOAH, Neurobiology of Adult Health; PIP, Pittsburgh Imaging Project; and SBP, systolic blood pressure.

[95% CI, 0.08–0.38]; *lnVR*=0.34 [95% CI, 0.05–0.60]). These expected statistical differences were likely attributable to interdevice variability and underscore the need for harmonizing these variables across cohorts.

Next, we assessed the associations between CA-IMT, SBP reactivity metrics, and CVD risk factors. As shown in Figure 1, greater CVD risk (as per the 10-year ASCVD score) correlated positively with CA-IMT (PIP: $r(300)=0.32$, $q<0.001$; NOAH: $r(283)=0.388$, $q<0.001$), as well as positively with SBP_AUC$_g$ (PIP: $r(296)=0.286$, $q<0.001$; NOAH: $r(251)=0.251$, $q<0.001$). Similar findings were observed for several other CVD risk factors; however, these associations did reliably replicate across the PIP and NOAH cohorts. Notably, SBP reactivity as indexed by ΔSBP did not appear to reliably correlate with the 10-year ASCVD risk factor (PIP: $r(297)=-0.01$, $q=0.928$; NOAH: $r(245)=0.047$, $q=0.592$). A similar situation was observed for SBP_AUC$_i$ (PIP: $r(296)=-0.012$, $q=0.927$; NOAH: $r(251)=0.093$, $q=0.227$). As a result, and following the preregistration plan, only comparisons of predicted versus observed values using SBP_AUC$_g$ as a mediator between stressor-evoked fMRI activity and CA-IMT were retested while controlling for prevailing levels of CVD risk indexed by ASCVD. For completeness, pairwise correlations between all these variables using the combined sample (PIP+NOAH) can be found in Figure S3, with similar conclusions reached as per each study.

Main Effects of the Stressor-Evoked fMRI Tasks

Stressor-evoked activation patterns were calculated as contrasts in average brain activity between incongruent and congruent trial conditions in both the Stroop task and MSIT, and for each cohort (PIP and NOAH). Areas typically implicated in conflict processing were found to be engaged (see Figure 2). This mainly involved positive activation of the dorsomedial prefrontal cortex, anterior cingulate cortex, anterior insula, parietal cortex, basal ganglia, thalamus, and cerebellum, and the negative activation of areas included in the default-mode network, encompassing the ventromedial prefrontal cortex, perigenual anterior cingulate cortex, posterior cingulate cortex, and precuneus. Overall, there was a large voxel-wise spatial similarity in activation patterns (Pearson correlation $r>0.8$) between tasks in PIP, and between cohorts for the Stroop task. Spatial similarity rates weakened when the activation pattern of MSIT in NOAH was evaluated, as a consequence of an overall decrease in observed effect sizes that particularly affected the lack of presence of significantly deactivated areas, that is, in the default-mode network (eg, the medial prefrontal and posterior cingulate cortex; Figure S4). This finding can be further understood by comparing the participants' behavior during MSIT across both cohorts. For example, a comparison can be made for the accuracy in correct responses of each

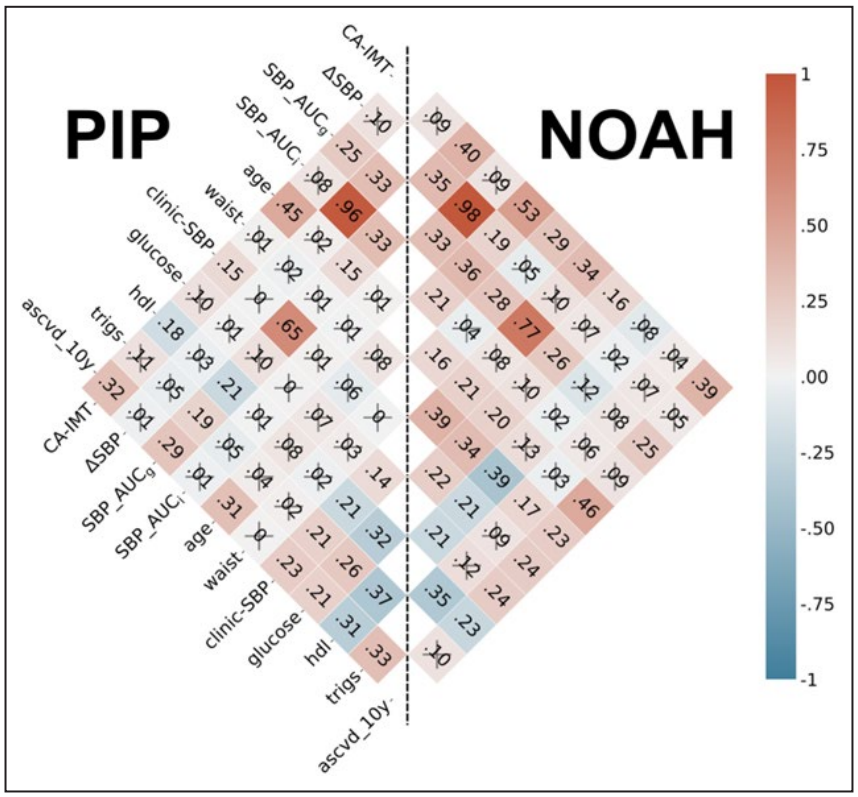

Figure 1. Correlogram.
A correlogram involving the main variables in our mediation framework and several cardiovascular disease risk factors. Colors and annotations display the strength of their associations as measured by Pearson correlation coefficients. An X represents those associations whose *P* values after false discovery rate correction were above the significance level α=0.05. ascvd_10y indicates 10-year atherosclerosis cardiovascular disease risk score; AUC_g, area under the curve with respect to the ground; AUC_i, area under the curve with respect to increase; CA-IMT, carotid artery intima-media thickness; hdl, high-density lipoprotein; NOAH, Neurobiology of Adult Health; PIP, Pittsburgh Imaging Project; SBP, systolic blood pressure; and trigs, triglycerides.

participant based on their choices during the tasks (a word selection in Stroop, a number selection in MSIT). Given that they serve as a control condition, high average performance should be observed across the congruent trials relative to the more challenging incongruent trials. However, although PIP participants did show the expected high accuracy (percentage of correct responses) during the congruent (91.08±7.41%) compared with the incongruent (56.05±9.09%) condition, this difference was considerably smaller for NOAH participants (congruent: 64.25±11.38%; incongruent: 53.92±2.51%) as attributable to the difference in the task structure/design. Therefore, relative to PIP participants, those in the NOAH cohort performed approximately 27% less accurately on average during congruent MSIT trials, resulting in similar decreased BOLD activity of the default-mode network relative to incongruent trials and in contrast to what occurs in the PIP cohort. Combat harmonization of the task-averaged activation patterns across both cohorts reduced (but did not entirely eliminate) these spatial differences (see Figure S5).

Prediction of CA-IMT From Stressor-Evoked Brain Activation Patterns and Mediated by Cardiovascular Reactivity

A mediation analysis using L2-penalized (ie, ridge) principal component regressions tested the association between stressor-evoked brain activity (input variable; X) and CA-IMT (outcome variable; Y) mediated by several cardiovascular reactivity measures: ΔSBP, SBP_AUC_g, and SBP_AUC_i (mediator variable; M). Figure 3 and Table 2 show that a significant association, in the holdout test sets, as indicated by the average coefficient of determination R^2 and 95% CIs, was found in the X-to-Y path for the 3 mediators, as well as in the X-to-M path and the [X+M]-to-Y path. Prediction performances summarized by Pearson correlation coefficients can be found in Table S1. In addition, predicted versus

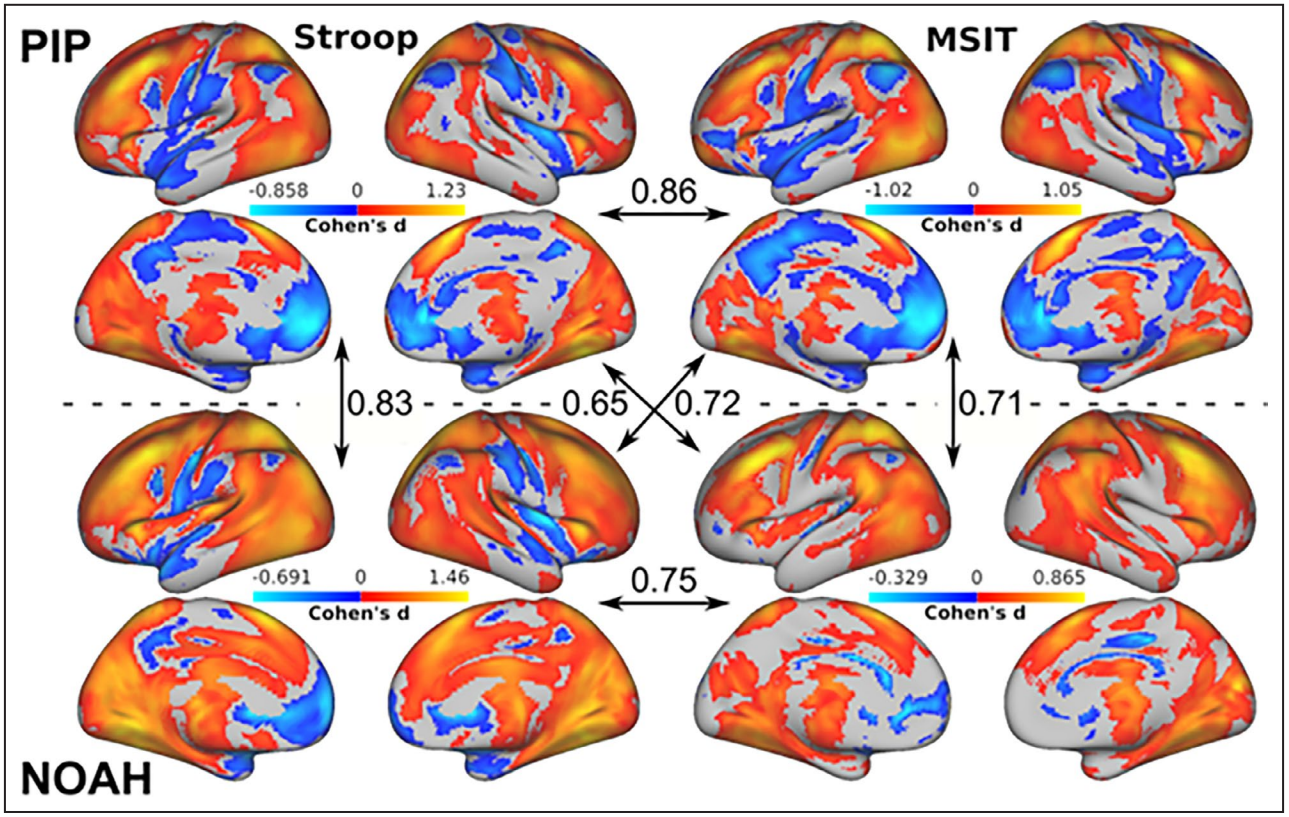

Figure 2. Main effects.
For each cohort (PIP and NOAH), the stressor-evoked brain activation patterns at the group level and in terms of the Cohen *d* effect size measure in both fMRI tasks (Stroop and MSIT). Only effects whose *P* value is <0.05 after false discovery rate correction and with a cluster size threshold of *k*>50 voxels are displayed. Orange colors represent greater average activity in the incongruent condition compared with the congruent condition, and blue colors represent the opposite. The arrows indicate the spatial similarity between activation patterns as measured by Pearson correlations. fMRI indicates functional magnetic resonance imaging; MSIT, multisource interference task; NOAH, Neurobiology of Adult Health; and PIP, Pittsburgh Imaging Project.

observed values across the different cross-validation repeats scatter plots are displayed in Figures S6, S7, and S8. As noted in the Methods section, the stratification in M and Y within each mediation analysis led to different data partitions and therefore to slightly different prediction rates in the X-to-Y path, although this model did not involve the mediator. Nonetheless, they all remained within the same CIs.

The previous results showed a generalizable effect for each model that comprises our mediation analysis framework. However, as shown in Figure 3 and Table 2, only SBP_AUC$_g$ had a sizeable and reliable mediation effect ($R^2_{med} = 0.073$ [95% CI, 0.070–0.076]), whereas it was substantially smaller for ΔSBP ($R^2_{med} = 0.005$ [95% CI, 0.005–0.006]) and SBP_AUC$_i$ ($R^2_{med} = 0.004$ [95% CI, 0.004–0.005]). This can be easily understood by the small variability explained by the latter 2 mediators in the M-to-Y path (ΔSBP: 0.009 [95% CI, 0.009–0.01]; SBP_AUC$_i$: 0.008 [95% CI, 0.007–0.009]; see Figure 3 and Table 2), and their lack of significant association with CA-IMT (see Figures S6 and S8), thereby violating the conditions necessary for mediation; additionally, R^2_{med} is negative if $R^2_{M\rightarrow Y} = 0$. As a consequence, we concluded that ΔSBP and SBP_AUC$_i$ could not represent viable mediators, so further analyses concentrated exclusively on SBP_AUC$_g$ in testing mediation effects between stressor-evoked brain activation and CA-IMT.

For completeness, we repeated the same analysis using L1-penalized (i.e., lasso) principal component regressions and found similar results, although with an overall decrease in effect sizes (see Figures S9, S10, and S11). Thus, findings appear to not depend on the type of penalty applied in modeling.

After conducting bootstrapping (5000 resamples) and correcting for multiple testing using a false discovery rate of 0.05, we identified 10 significant principal components for the indirect effects (i.e., *a*×*b* products), and no significant principal components for the direct effects (*c*' coefficients). In the mediation analysis context, this suggests that the association between stressor-evoked brain activation and CA-IMT appears to be fully mediated by SBP_AUC$_g$.

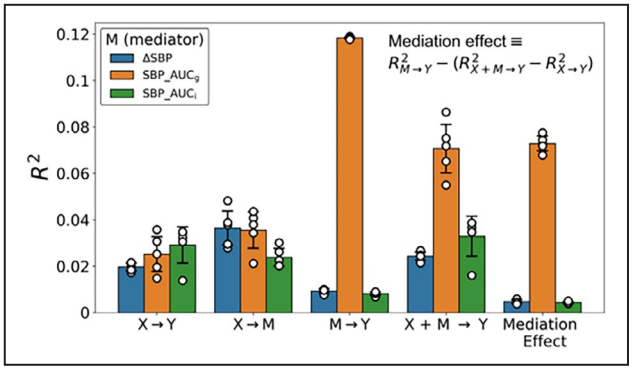

Figure 3. Out-of-sample performances.
For each possible mediator variable (M), the out-of-sample performance using an L2-penalized principal component regression and applied to the different paths in the mediation analysis framework. Here, the input variable (X) is voxel-wise responses, and the output variable (Y) is CA-IMT. Each dot represents the coefficient of determination calculated from the observed vs predicted values generated from a particular run of the nested cross-validation procedure. In addition, bars and error bars display the average and the 95% CIs across these values. AUC_g indicates area under the curve with respect to the ground; AUC_i, area under the curve with respect to increase; CA-IMT, carotid artery intima-media thickness; and SBP, systolic blood pressure.

When we transformed these 10 significant components back to the voxel space, we found a (mediated) positive association in areas involving particularly the insula, thalamus, ventromedial prefrontal cortex, anterior cingulate cortex, superior parietal lobe, and vermis (see encoding weight maps in Figure 4). Since the *b* coefficient was always positive, this means that SBP_AUC_g increases as incongruency-related brain responses in these areas increase. Conversely, we observed a (mediated) negative association in the dorsomedial prefrontal cortex, angular gyrus, amygdala, cerebellum, and brain stem. Therefore, when incongruency-related brain patterns increase in these areas, SBP_AUC_g tends to decrease. Interestingly, there appeared to be a lateralization of the amygdala, because positive associations take place in the left hemisphere and negative associations in the right hemisphere. The loadings for these 10 significant components, ordered by importance and separated into positive and negative contributions to the indirect effects, can be found in Figure S12.

Finally, Figure S13 displays the brain patterns of encoding weights from the X-to-M path for each mediator variable. We include them here for comparison, retaining all their principal components information. As expected, due to the high correlation between ΔSBP and SBP_AUC_i (see Figure 1 for the correlation values in both cohorts), their weight maps in the X-to-M path also exhibit a large spatial similarity (r=0.96). In contrast, their spatial similarity with the weight map for SBP_AUC_g substantially decreased (ΔSBP: r=0.42, SBP_AUC_i: r=0.43). These differences appear to be triggered by an overall presence of negative associations in the dorsomedial prefrontal cortex, anterior cingulate cortex and angular gyrus for SBP_AUC_g, unlike ΔSBP and SBP_AUC_i where these associations are positive.

Ancillary Testing

We have shown that SBP_AUC_g appears to significantly mediate an association between stressor-evoked brain activation and CA-IMT. In this scenario, a small deviation from the sequential ignorability assumptions could be observed, as measured by $\rho=cor(\varepsilon_{X->M}, \varepsilon_{XM->Y})=0.213$, that is, the correlation between the errors in the X-to-M path and the errors in the [X+M]-to-Y path.[58] Here these errors were based on the out-of-sample predictions and the reported value of ρ on the average over the different cross-validation runs. We next tested whether this mediation effect could be explained by prevailing levels of cardiovascular disease risk factors.

An overall decrease in explained variability was observed after including the 10-year ASCVD risk score as a control variable in the scenario involving SBP_AUC_g as a mediator. Nevertheless, associations remained significant for the X-to-M path (R^2=0.022 [95% CI, 0.014–0.022]) and the [X+M]-to-Y path (R^2=0.039 [95% CI, 0.027–0.05]). Only for the X-to-Y path, 2 repetitions of the cross-validation procedure no longer yielded a significant correlation in observed versus predicted values. Altogether, a significant mediation effect was still observed ($R^2_{med} = 0.046$ [95% CI, 0.042–0.049]). Therefore, we can conclude that the prevailing values

Table 2. Coefficients of Determination (R^2)

Statistical Paths	ΔSBP	SBP_AUC_g	SBP_AUC_i
X-to-Y path	0.02 [0.018–0.021]	0.025 [0.018–0.033]	0.029 [0.021–0.037]
X-to-M path	0.036 [0.029–0.044]	0.036 [0.028–0.043]	0.024 [0.02–0.028]
M-to-Y path	0.009 [0.009–0.01]	0.118 [0.118–0.119]	0.008 [0.007–0.009]
[X+M]-to-Y path	0.024 [0.023–0.026]	0.071 [0.06–0.081]	0.033 [0.025–0.041]
Mediation effect	0.005 [0.004–0.006]	0.073 [0.070–0.076]	0.004 [0.004–0.005]

AUC_g, area under the curve with respect to ground; AUC_i, area under the curve with respect to increase; and SBP, systolic blood pressure.

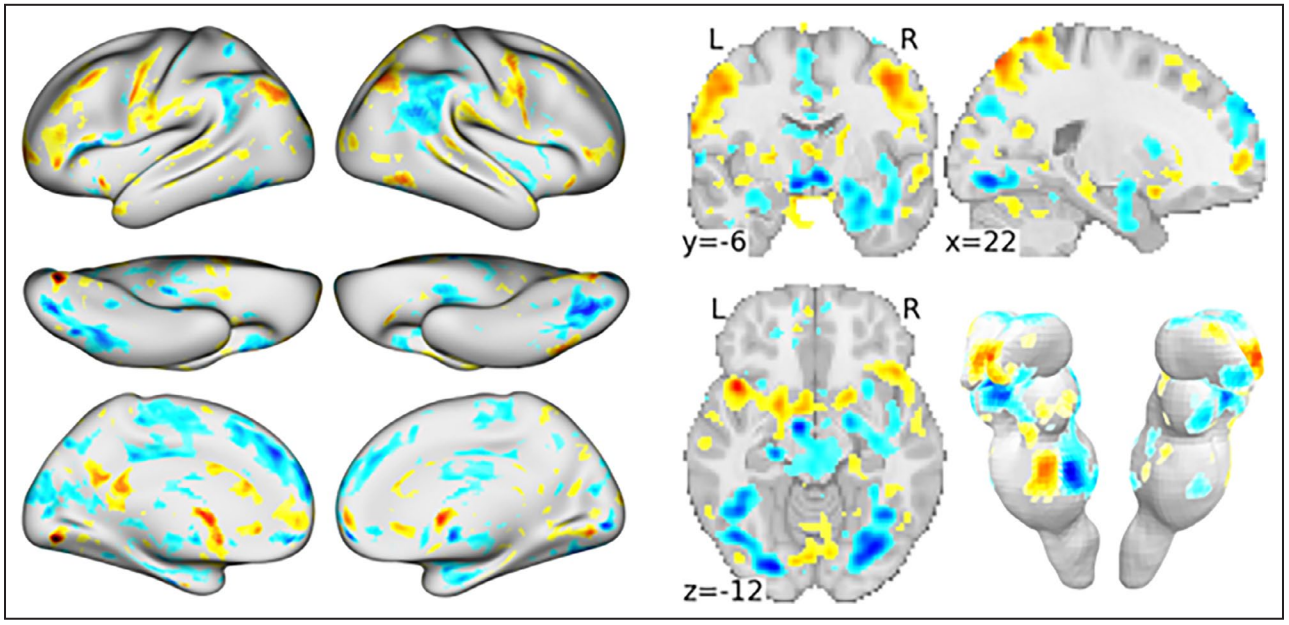

Figure 4. Encoding weight maps of indirect effects.
For the scenario with SBP_AUC$_g$ as mediator, the encoding weight maps obtained from transforming back to voxel space those principal components whose *a*×*b* products were significant based on bootstrapping (5000 resamples) and after correcting for a false discovery rate of 0.05. Warm and cool colors represent a positive and negative mediated association between stressor-evoked brain activity and CA-IMT, respectively. For visualization purposes, only weights with |z|>1 after spatial standardization are displayed. AUC$_g$ indicates area under the curve with respect to the ground; CA-IMT, carotid artery intima-media thickness; L, left; R, right; and SBP, systolic blood pressure.

of CVD risk factors do not drive this mediation effect between stressor-evoked brain activity and CA-IMT.

We performed a sensitivity analysis by concentrating exclusively on subjects with low in-scanner head motion, defined as having an average framewise displacement <0.5 mm in both fMRI tasks. This resulted in the exclusion of 27 subjects (23 belonging to PIP, and 4 to NOAH). A mild improvement in performance rates was overall observed (see Figure S14), although conclusions previously reached remained the same.

Last, in exploratory analyses that were not preregistered, we evaluated metrics of DBP reactivity as correlates of CA-IMT and possible mediators between stressor-evoked fMRI activity and CA-IMT. Here, we first observed that SBP and DBP reactivity metrics were moderately to highly correlated, with *r* values ranging from 0.63 to 0.83. DBP metrics also exhibited patterns of association with CA-IMT that were comparable to those for DBP reactivity, with DBP_AUC$_g$ exhibiting the highest correlation with CA-IMT relative to change and AUC$_i$ metrics (*r* values=0.04 and 0.05, respectively). Finally, mediation tests confirmed that only DBP_AUC$_g$ exhibited a reliable indirect effect in the mediated association between stressor-evoked fMRI activity and CA-IMT (see Figure S15 and Tables S2 and S3).

DISCUSSION

In this study we tested whether whole-brain hemodynamic activity patterns, evoked by 2 aversive information conflict tasks (Stroop and MSIT), were associated with CA-IMT, a vascular marker of preclinical atherosclerosis. We also tested whether this association was statistically mediated by 3 different measures of cardiovascular, principally SBP, reactivity. To accomplish this, we used a mult-cohort data set comprising ≈600 subjects and the combination of harmonization techniques and penalized principal component regressions to estimate generalizable out-of-sample predictions from a repeated nested cross-validation procedure. Within a mediation analysis framework, we found that stressor-evoked brain activity patterns explained ≈2% of total variability of CA-IMT (the X-to-Y path). The same activation patterns were able to predict cardiovascular reactivity (the X-to-M path), with a variability between 4% and 2% depending on the mediator variable. In addition, when brain activation patterns and cardiovascular reactivity were considered together (the [X+M]-to-Y path), prediction rates of CA-IMT increased, reaching the maximum explained variability (around 8%) for the case of SBP_AUC$_g$ as a mediator. Collectively, the present findings suggest that the association between stressor-evoked brain activity and CA-IMT is likely to

be mediated most reliably by SBP_AUC$_g$, and mainly via the activation of areas such as the insula, thalamus, ventromedial prefrontal cortex, and superior parietal lobe, and the deactivation in the dorsomedial prefrontal cortex, angular gyrus, amygdala, cerebellum, and brain stem. Importantly, the present results could not be explained by prevailing levels of cardiovascular disease risk or excessive head motion, suggesting that the observed associations may not be artifactual. These novel findings are consistent with the possibility that part of the relationship between stressor-evoked brain activity and preclinical atherosclerosis may be accounted for by individual differences in corresponding levels of stressor-evoked cardiovascular reactivity.

Our study builds upon a growing body of evidence for the possible brain systems and physiological pathways that may link psychological stress to preclinical atherosclerosis and CVD risk. We previously showed, for example, that brain activity patterns evoked by 2 different sets of unpleasant emotional stimuli were able to successfully predict individual differences of CA-IMT, explaining 1% to 3% of interindividual variability.[51] Important brain regions for these predictions included the insula, hypothalamus, brainstem, and areas of the anterior cingulate and medial prefrontal cortices. Here, our brain activity patterns emerging from an fMRI stressor battery were able to explain a roughly similar variability of CA-IMT (≈2%) across individuals and particularly engaged similar brain areas. Thus, our results appear to agree with evidence of an interdependence between executive functions, contextual appraisals, and affective processes,[60–63] which here is also reflected in their similar relationship with preclinical atherosclerosis. It remains to be tested whether the integration across all these different task paradigms that engage such interdependent processes could boost the prediction of individual differences in cardiovascular disease risk, similar to what was found for blood pressure reactivity using the same 2 tasks used here.[34] Importantly, integrating patterns of fMRI activity across different task paradigms could be an alternative to combining different neuroimaging modalities, because the latter has not been shown to improve the prediction of preclinical atherosclerosis.[64]

We also demonstrated that stressor-evoked brain activity relates to acute changes in SBP, which was consistent across the 3 cardiovascular reactivity measures that we tested. Our supplementary results using L1-penalized principal component regression and involving ΔSBP as the outcome variable (minimum r=0.206, maximum r=0.256; see Figure S9) followed those previously reported using 1 of the cohorts in the data set,[34] although with a slight reduction in prediction performance (but within the same levels of CIs). This is likely due to the increased sample size that tends to stabilize effect sizes to their generalizable true value.[65,66] Nevertheless, the obtained prediction rates were still small. It has been argued that an explanation for such small effect sizes is that task-fMRI measures are not reliable enough.[67] However, this argument is still in debate.[68] Here we used a sample size much larger than those previously reported,[67] and used task-aggregated multivariate patterns that have been demonstrated to increase reliability for the prediction of individual differences.[36] Therefore, albeit small, the observed generalizable associations of stressor-evoked brain activation patterns with preclinical atherosclerosis and cardiovascular reactivity may be likely to approximate their true value. It is also important to note that peripheral blood pressure responses are not entirely determined by brain systems for visceral control: such responses are likely to be additionally influenced by variation in autonomic outflow, peripheral autonomic receptor density and sensitivity (eg, α- and β-adrenergic receptor density and sensitivity), as well as other vascular determinants that could also account for non–brain-related and unexplained variance in cardiovascular reactivity across individuals.[69]

Notably, among the 3 cardiovascular reactivity measures tested, only SBP_AUC$_g$ appeared to mediate a reliable association between stressor-evoked brain activity and CA-IMT. This also appeared to be the case in exploratory analyses using DBP reactivity metrics (Data S1). We speculate that this is due to this cardiovascular reactivity variable, namely SBP_AUC$_g$, being the only one exhibiting a moderately sizable association with CA-IMT, as shown by the results for the M-to-Y path in Figure 3. In our context, AUC$_g$ summarizes the total BP reactivity output under a series of events, here comprising BP throughout magnetic resonance imaging testing, whereas AUC$_i$ is possibly more related to the sensitivity of the measure to variable changes and peak values over time.[46] Because the latter involves BP changes with respect to the baseline in both incongruent and congruent conditions, and considering that the time separation between successive BP events throughout the task sequences is always the same, it is not surprising that it almost perfectly correlates with ΔBP, which involves average changes with respect to the baseline only within the incongruent condition (for SBP, PIP: 0.98, NOAH: 0.96, see Figure 1). It might be the case that each area under the curve-based cardiovascular reactivity measure corresponds to a particular feature of individual differences in preclinical atherosclerosis; for example overall intensity, as similarly encoded by AUC$_g$-based measures, appears to mostly correlate with cross-sectional values, whereas acute reactions, as similarly encoded by AUC$_i$-based measures, appear to be more important in explaining longitudinal changes over time.[70] By these and related considerations, it has been recommended to include all such metrics when analyzing data with repeated

measures of stress physiology.[46] Nevertheless, in regard to the variance in CA-IMT accounted for by reactivity measures in preregistered analyses, such as ΔSBP (and SBP_AUC_i in extent), which we found to exhibit an average R^2=0.009 (95% CI, 0.009–0.01) (or r=0.097 [95% CI, 0.094–0.101]), it is important to highlight that this closely compares to the meta-analytic effect size of the association of BP reactivity and CVD risk, r=0.096, reported previously.[14] Although small in magnitude, our observed effect sizes thus appear to align with cumulative evidence and implicate additional biological pathways beyond cardiovascular reactivity (eg, inflammatory, neuroendocrine, mitochondrial) that may link stress-related brain functionality to CVD risk, as well as underscoring the need in the field for large sample sizes and cross-validation methods.

Furthermore, in our bootstrapping analysis applied to the scenario with SBP_AUC_g as the mediator, we found that this mediation effect was observed along 10 principal components computed from multivariate brain activation patterns. Strikingly, the coefficients of each of these components in the X-to-Y path, that is, the total effect (or c coefficients) did not show a statistical significance after correcting for multiple testing. Is it possible then that a mediation effect exists even in the absence of total effects? In the original casual step approach to mediation analysis, the first requirement for a possible mediation effect was that the X-to-Y path should be significant.[48,71,72] However, the necessity of this has been challenged over time.[73,74] Looking into our case, each principal component from the stressor-evoked brain activity patterns was a potential candidate for a mediating effect. We found that the estimated coefficients for these indirect effects (ie, the $a \times b$ products) had all roughly opposite signs, which is one of the possible explanations as to how a mediation effect in the absence of an overall association may occur.[75] This might be due to the fact that principal component analysis basically finds orthogonal axes, and therefore their estimated coefficients also reflect this orthogonality in terms of exhibiting opposite signs in their association with the outcome variable, although we acknowledge that this assertion requires further exploration.

Also notable is the encoding weight pattern of the significant indirect effects, which included brain regions such as the ventromedial prefrontal cortex, anterior cingulate cortex, insula, and amygdala. These areas are part of what has been termed a visceral control network, which is proposed to be involved in mediating psychological stress appraisals and simultaneously controlling cardiovascular physiology mechanistically via their influence over autonomic and related determinants of BP (eg, baroreflex suppression), with alterations in this network being hypothesized to influence risk for cardiovascular disease.[9] These brain systems have also been recently described as belonging to an interoceptive-allostatic brain network for regulating peripheral physiology by predictive or anticipatory processes.[76,77] Along similar lines, our results appear to provide evidence for a pathway whereby increased brain activity in systems encompassed by these networks associates with larger rises in stressor-evoked systolic blood pressure and preclinical atherosclerosis across people. Interestingly, we also observed a lateralization in the role of the amygdala, with increased activity in the left and right hemisphere to be positively and negatively associated with cardiovascular reactivity, respectively. Asymmetry in the activation of the amygdala has been exhaustively reported (see[78] and references therein). We note further that several possible mechanistic pathways other than BP per se (eg, hematopoietic tissue activity, arterial inflammation) may also be involved in linking stress-related neural activity to CVD risk.[79] For an updated summary of the possible neural mechanisms linking psychological stress to CVD risk, we refer readers to a recent comprehensive review.[80]

Finally, several limitations of our study should be noted. First, our cohorts (PIP and NOAH) included predominantly white individuals who were relatively well educated and free of major chronic illnesses and medication regimens that could have confounded interpretations of preclinical atherosclerosis and cardiovascular reactivity markers. As a result, whether our findings are relevant to demographically diverse individuals and clinical populations is still unclear. Yet, we have made the multivariate predictive patterns reported here publicly available, so they could be eventually tested in other populations and used as predictors in tasks involving different clinical and preclinical outcomes. Second, our results were obtained from task-based activation metrics and therefore did not involve some of the methodological and psychometric advantages that morphological, task-free (or resting state)-based measures could hold in the prediction of preclinical atherosclerosis, reactivity, and other cardiovascular disease risk factors.[81–84] Third, to quantify mediation effects in an out-of-sample framework, we resorted to a explained variance-based measure for mediation analysis, which has its own limitations.[85] Efforts to find the optimal measure of effect size for mediation analysis continues to be an active area of research.[86] Fourth, the present study did not statistically test possible moderators of the mediated associations reported here (eg, moderating influences of sex at birth, gender, chronic psychosocial stress, socioeconomic position, health status, etc.). For example, from a diathesis-stress perspective, it may be possible that higher levels of prevailing cardiovascular risk, as reflected in composite risk indicators,[87] could plausibly increase vulnerability to stress-related neural and physiological influences on preclinical vascular disease (see Spencer et al[88]). Future studies may explore moderated mediation if appropriate conditions (eg, enough statistical power) are met, and publicly available data from this report might facilitate initial exploratory testing. Last,

causal inferences from the present observations are precluded because they are cross-sectional. Preclinical vascular disease, as reflected in CA-IMT, may have central influences that manifest as alterations in cerebral blood flow or neural-hemodynamic coupling.[89,90] In these regards, BP and related indicators of preclinical vascular disease are established risk factors for adverse central nervous system outcomes, including neurocognitive decline and neuropathology.[91–95] Future longitudinal and interventional studies may thus help to adjudicate the temporal or causal relationships of stressor-evoked fMRI and BP reactivity to CA-IMT. In addition, the interpretation of the different causal effects may be influenced by deviations in the sequential ignorability assumptions. Statistically, we found these deviations to be small and attempted to control for confounding effects by accounting for prevailing levels of CVD risk as a plausible covariate. However, future research should investigate the effects of other potential unmeasured confounders not included in our study.

Despite these limitations, the present findings provide novel cross-validated, predictive, and machine-learning evidence for the possible mediating role of stressor-evoked cardiovascular reactivity in linking multivariate brain responses to acute psychological stressors and a vascular marker of preclinical atherosclerosis.diovascular reactivity in linking multivariate brain responses to acute psychological stressors and a vascular marker of preclinical atherosclerosis.

ARTICLE INFORMATION

Received February 13, 2024; accepted September 6, 2024.

Affiliations

Department of Psychology and Neuroscience Institute, Carnegie Mellon University, Pittsburgh, PA (J.R., T.D.V.); School of Data Science, University of Virginia, Charlottesville, VA (J.R.); Department of Psychology (C.M.D., M.R.S., T.W.K., R.L.L., P.J.G.), Department of Epidemiology (T.E.K., E.B.) and School of Medicine, University of Pittsburgh, PA (A.I.S.).

Acknowledgments

We thank S. Boyko for her role in data collection and J. Lower for her role in data management.

Sources of Funding

The research reported here was supported by the National Heart, Lung, and Blood Institute of the National Institutes of Health under grants P01HL040962 and R01HL089850. The content is solely the responsibility of the authors and does not necessarily represent the official views of the National Institutes of Health.

Disclosures

None.

Supplemental Material

Data S1

REFERENCES

1. Crosswell AD, Epel ES, Mendes WB, Prather AA. Improving the language specificity of stress in psychological and population health science. *Psychosom Med*. 2022;84:643–644. doi: 10.1097/PSY.0000000000001090
2. Epel ES, Crosswell AD, Mayer SE, Prather AA, Slavich GM, Puterman E, Mendes WB. More than a feeling: a unified view of stress measurement for population science. *Front Neuroendocrinol*. 2018;49:146–169. doi: 10.1016/j.yfrne.2018.03.001
3. Cohen S, Gianaros PJ, Manuck SB. A stage model of stress and disease. *Perspect Psychol Sci*. 2016;11:456–463. doi: 10.1177/1745691616646305
4. Brindle RC, Ginty AT, Phillips AC, Carroll D. A tale of two mechanisms: a meta-analytic approach toward understanding the autonomic basis of cardiovascular reactivity to acute psychological stress: autonomic basis of cardiovascular reactivity. *Psychophysiology*. 2014;51:964–976. doi: 10.1111/psyp.12248
5. Dimsdale JE. Psychological stress and cardiovascular disease. *J Am Coll Cardiol*. 2008;51:1237–1246. doi: 10.1016/j.jacc.2007.12.024
6. Shah SM, Meadows JL, Burg MM, Pfau S, Soufer R. Effects of psychological stress on vascular physiology: beyond the current imaging signal. *Curr Cardiol Rep*. 2020;22:156. doi: 10.1007/s11886-020-01406-x
7. Steptoe A, Kivimäki M. Stress and cardiovascular disease. *Nat Rev Cardiol*. 2012;9:360–370. doi: 10.1038/nrcardio.2012.45
8. Kamarck TW, Lovallo WR. Cardiovascular reactivity to psychological challenge: conceptual and measurement considerations. *Psychosom Med*. 2003;65:9–21. doi: 10.1097/01.PSY.0000030390.34416.3E
9. Gianaros PJ, Jennings JR. Host in the machine: a neurobiological perspective on psychological stress and cardiovascular disease. *Am Psychol*. 2018;73:1031–1044. doi: 10.1037/amp0000232
10. Gianaros PJ, Wager TD. Brain-body pathways linking psychological stress and physical health. *Curr Dir Psychol Sci*. 2015;24:313–321. doi: 10.1177/0963721415581476
11. Ginty AT, Kraynak TE, Fisher JP, Gianaros PJ. Cardiovascular and autonomic reactivity to psychological stress: neurophysiological substrates and links to cardiovascular disease. *Auton Neurosci*. 2017;207:2–9. doi: 10.1016/j.autneu.2017.03.003
12. Koban L, Gianaros PJ, Kober H, Wager TD. The self in context: brain systems linking mental and physical health. *Nat Rev Neurosci*. 2021;22:309–322. doi: 10.1038/s41583-021-00446-8
13. Kamarck TW, Debski TT, Manuck SB. Enhancing the laboratory-to-life generalizability of cardiovascular reactivity using multiple occasions of measurement. *Psychophysiology*. 2000;37:533–542. doi: 10.1111/1469-8986.3740533
14. Chida Y, Steptoe A. Greater cardiovascular responses to laboratory mental stress are associated with poor subsequent cardiovascular risk status: a meta-analysis of prospective evidence. *Hypertension*. 2010;55:1026–1032. doi: 10.1161/HYPERTENSIONAHA.109.146621
15. Turner AI, Smyth N, Hall SJ, Torres SJ, Hussein M, Jayasinghe SU, Ball K, Clow AJ. Psychological stress reactivity and future health and disease outcomes: a systematic review of prospective evidence. *Psychoneuroendocrinology*. 2020;114:104599. doi: 10.1016/j.psyneuen.2020.104599
16. Carroll D, Ginty AT, Der G, Hunt K, Benzeval M, Phillips AC. Increased blood pressure reactions to acute mental stress are associated with 16-year cardiovascular disease mortality: stress reactivity and cardiovascular disease mortality. *Psychophysiology*. 2012;49:1444–1448. doi: 10.1111/j.1469-8986.2012.01463.x
17. Krantz DS, Manuck SB. Acute psychophysiologic reactivity and risk of cardiovascular disease: a review and methodologic critique. *Psychol Bull*. 1984;96:435–464. doi: 10.1037/0033-2909.96.3.435
18. Manuck SB. Cardiovascular reactivity in cardiovascular disease: "once more unto the breach". *Int J Behav Med*. 1994;1:4–31. doi: 10.1207/s15327558ijbm0101_2
19. Manuck SB, Kaplan JR, Matthews KA. Behavioral antecedents of coronary heart disease and atherosclerosis. *Arteriosclerosis*. 1986;6:2–14. doi: 10.1161/01.ATV.6.1.2
20. Manuck SB, Kasprowicz AL, Monroe SM, Larkin KT, Kaplan JR. Psychophysiologic reactivity as a dimension of individual differences. In: Schneiderman N, Weiss SM, Kaufmann PG, eds *Handbook of Research Methods in Cardiovascular Behavioral Medicine*. Boston, MA: Springer US; 1989:365–382.
21. Manuck SB, Marsland AL, Kaplan JR, Williams JK. The pathogenicity of behavior and its neuroendocrine mediation: an example from coronary artery disease. *Psychosom Med*. 1995;57:275–283. doi: 10.1097/00006842-199505000-00009

22. Schwartz AR, Gerin W, Davidson KW, Pickering TG, Brosschot JF, Thayer JF, Christenfeld N, Linden W. Toward a causal model of cardiovascular responses to stress and the development of cardiovascular disease. *Psychosom Med*. 2003;65:22–35. doi: 10.1097/01.PSY.0000046075.79922.61
23. Sharpley CF. Psychosocial stress-induced heart rate reactivity and atherogenesis: cause or correlation? *J Behav Med*. 1998;21:411–432. doi: 10.1023/A:1018734925282
24. Treiber FA, Kamarck T, Schneiderman N, Sheffield D, Kapuku G, Taylor T. Cardiovascular reactivity and development of preclinical and clinical disease states. *Psychosom Med*. 2003;65:46–62. doi: 10.1097/00006842-200301000-00007
25. Lasheras JC. The biomechanics of arterial aneurysms. *Annu Rev Fluid Mech*. 2007;39:293–319. doi: 10.1146/annurev.fluid.39.050905.110128
26. Beere PA, Glagov S, Zarins CK. Retarding effect of lowered heart rate on coronary atherosclerosis. *Science*. 1984;226:180–182. doi: 10.1126/science.6484569
27. Gordon D, Guyton JR, Karnovsky MJ. Intimal alterations in rat aorta induced by stressful stimuli. *Lab Investig J Tech Methods Pathol*. 1981;45:14–27.
28. Shafi S, Cusack NJ, Born GV. Increased uptake of methylated low-density lipoprotein induced by noradrenaline in carotid arteries of anaesthetized rabbits. *Proc R Soc Lond B Biol Sci*. 1989;235:289–298. doi: 10.1098/rspb.1989.0001
29. Cooper DC, Katzel LI, Waldstein SR. Cardiovascular reactivity in older adults. In: Aldwin CM, Park CL, Spiro A III, eds *Handbook of Health Psychology and Aging*. New York, NY, US: The Guilford Press; 2007:142–164.
30. Lipman RD, Grossman P, Bridges SE, Hamner JW, Taylor JA. Mental stress response, arterial stiffness, and baroreflex sensitivity in healthy aging. *J Gerontol A Biol Sci Med Sci*. 2002;57:B279–B284. doi: 10.1093/gerona/57.7.B279
31. Sherwood A, Johnson K, Blumenthal JA, Hinderliter AL. Endothelial function and hemodynamic responses during mental stress. *Psychosom Med*. 1999;61:365–370. doi: 10.1097/00006842-199905000-00017
32. Osborne MT, Shin LM, Mehta NN, Pitman RK, Fayad ZA, Tawakol A. Disentangling the links between psychosocial stress and cardiovascular disease. *Circ Cardiovasc Imaging*. 2020;13:e010931. doi: 10.1161/CIRCIMAGING.120.010931
33. Banihashemi L, Sheu LK, Midei AJ, Gianaros PJ. Childhood physical abuse predicts stressor-evoked activity within central visceral control regions. *Soc Cogn Affect Neurosci*. 2015;10:474–485. doi: 10.1093/scan/nsu073
34. Gianaros PJ, Sheu LK, Uyar F, Koushik J, Jennings JR, Wager TD, Singh A, Verstynen TD. A brain phenotype for stressor-evoked blood pressure reactivity. *J Am Heart Assoc*. 2017;6:e006053. doi: 10.1161/JAHA.117.006053
35. Lockwood KG, Marsland AL, Cohen S, Gianaros PJ. Sex differences in the association between stressor-evoked interleukin-6 reactivity and C-reactive protein. *Brain Behav Immun*. 2016;58:173–180. doi: 10.1016/j.bbi.2016.07.001
36. Sheu LK, Jennings JR, Gianaros PJ. Test–retest reliability of an fMRI paradigm for studies of cardiovascular reactivity: test–retest reliability of an fMRI paradigm. *Psychophysiology*. 2012;49:873–884. doi: 10.1111/j.1469-8986.2012.01382.x
37. Gianaros PJ, Rasero J, DuPont CM, Kraynak TE, Gross JJ, McRae K, Wright AGC, Verstynen TD, Barinas-Mitchell E. Multivariate brain activity while viewing and reappraising affective scenes does not predict the multiyear progression of preclinical atherosclerosis in otherwise healthy midlife adults. *Affect Sci*. 2022;3:406–424. doi: 10.1007/s42761-021-00098-y
38. Grundy SM, Stone NJ, Bailey AL, Beam C, Birtcher KK, Blumenthal RS, Braun LT, de Ferranti S, Faiella-Tommasino J, Forman DE, et al. 2018 AHA/ACC/AACVPR/AAPA/ABC/ACPM/ADA/AGS/APhA/ASPC/NLA/PCNA guideline on the management of blood cholesterol: a report of the American College of Cardiology/American Heart Association Task Force on Clinical Practice Guidelines. *Circulation*. 2019;139:e1046–e1081. doi: 10.1161/CIR.0000000000000625
39. R Core Team. *R: A Language and Environment for Statistical Computing*. Vienna: R Core Team; 2021. https://www.R-project.org
40. Goff DC, Lloyd-Jones DM, Bennett G, Coady S, D'Agostino RB, Gibbons R, Greenland P, Lackland DT, Levy D, O'Donnell CJ, et al. 2013 ACC/AHA guideline on the assessment of cardiovascular risk: a report of the American College of Cardiology/American Heart Association Task Force on Practice Guidelines. *Circulation*. 2014;129:S49–S73. doi: 10.1161/01.cir.0000437741.48606.98
41. Krieger N. Discrimination and health inequities. *Int J Health Serv*. 2014;44:643–710. doi: 10.2190/HS.44.4.b
42. Volpe VV, Dawson DN, Rahal D, Wiley KC, Vesslee S. Bringing psychological science to bear on racial health disparities: the promise of centering Black health through a critical race framework. *Transl Issues Psychol Sci*. 2019;5:302–314. doi: 10.1037/tps0000205
43. D'Agostino RB, Vasan RS, Pencina MJ, Wolf PA, Cobain M, Massaro JM, Kannel WB. General cardiovascular risk profile for use in primary care: the Framingham heart study. *Circulation*. 2008;117:743–753. doi: 10.1161/CIRCULATIONAHA.107.699579
44. Linden W, Earle TL, Gerin W, Christenfeld N. Physiological stress reactivity and recovery: conceptual siblings separated at birth? *J Psychosom Res*. 1997;42:117–135. doi: 10.1016/S0022-3999(96)00240-1
45. Llabre MM, Spitzer SB, Saab PG, Ironson GH, Schneiderman N. The reliability and specificity of delta versus residualized change as measures of cardiovascular reactivity to behavioral challenges. *Psychophysiology*. 1991;28:701–711. doi: 10.1111/j.1469-8986.1991.tb01017.x
46. Pruessner JC, Kirschbaum C, Meinlschmid G, Hellhammer DH. Two formulas for computation of the area under the curve represent measures of total hormone concentration versus time-dependent change. *Psychoneuroendocrinology*. 2003;28:916–931. doi: 10.1016/S0306-4530(02)00108-7
47. DuPont CM, Pressman SD, Reed RG, Manuck SB, Marsland AL, Gianaros PJ. An online Trier social stress paradigm to evoke affective and cardiovascular responses. *Psychophysiology*. 2022;59:e14067. doi: 10.1111/psyp.14067
48. Baron RM, Kenny DA. The moderator–mediator variable distinction in social psychological research: conceptual, strategic, and statistical considerations. *J Pers Soc Psychol*. 1986;51:1173–1182. doi: 10.1037/0022-3514.51.6.1173
49. Spisak T, Bingel U, Wager TD. Multivariate BWAS can be replicable with moderate sample sizes. *Nature*. 2023;615:E4–E7. doi: 10.1038/s41586-023-05745-x
50. Wager TD, Atlas LY, Leotti LA, Rilling JK. Predicting individual differences in placebo analgesia: contributions of brain activity during anticipation and pain experience. *J Neurosci*. 2011;31:439–452. doi: 10.1523/JNEUROSCI.3420-10.2011
51. Gianaros PJ, Kraynak TE, Kuan DC-H, Gross JJ, McRae K, Hariri AR, Manuck SB, Rasero J, Verstynen TD. Affective brain patterns as multivariate neural correlates of cardiovascular disease risk. *Soc Cogn Affect Neurosci*. 2020;15:1034–1045. doi: 10.1093/scan/nsaa050
52. Rieck J, Wrobel J, Porras AR, McRae K, Gowin JL. Neural signatures of emotion regulation. *Sci Rep*. 2024;14:1775. doi: 10.1038/s41598-024-52203-3
53. Poldrack RA, Huckins G, Varoquaux G. Establishment of best practices for evidence for prediction: a review. *JAMA Psychiatry*. 2020;77:534–540. doi: 10.1001/jamapsychiatry.2019.3671
54. Fairchild AJ, MacKinnon DP, Taborga MP, Taylor AB. R^2 effect-size measures for mediation analysis. *Behav Res Methods*. 2009;41:486–498. doi: 10.3758/BRM.41.2.486
55. Benjamini Y, Hochberg Y. Controlling the false discovery rate: a practical and powerful approach to multiple testing. *J R Stat Soc Ser B Methodol*. 1995;57:289–300. doi: 10.1111/j.2517-6161.1995.tb02031.x
56. Haufe S, Meinecke F, Görgen K, Dähne S, Haynes J-D, Blankertz B, Bießmann F. On the interpretation of weight vectors of linear models in multivariate neuroimaging. *NeuroImage*. 2014;87:96–110. doi: 10.1016/j.neuroimage.2013.10.067
57. Johnson WE, Li C, Rabinovic A. Adjusting batch effects in microarray expression data using empirical Bayes methods. *Biostatistics*. 2007;8:118–127. doi: 10.1093/biostatistics/kxj037
58. Imai K, Keele L, Tingley D. A general approach to causal mediation analysis. *Psychol Methods*. 2010;15:309–334. doi: 10.1037/a0020761
59. Power JD, Barnes KA, Snyder AZ, Schlaggar BL, Petersen SE. Spurious but systematic correlations in functional connectivity MRI networks arise from subject motion. *NeuroImage*. 2012;59:2142–2154. doi: 10.1016/j.neuroimage.2011.10.018
60. Gray JR, Braver TS, Raichle ME. Integration of emotion and cognition in the lateral prefrontal cortex. *Proc Natl Acad Sci*. 2002;99:4115–4120. doi: 10.1073/pnas.062381899
61. Storbeck J, Clore GL. On the interdependence of cognition and emotion. *Cognit Emot*. 2007;21:1212–1237. doi: 10.1080/02699930701438020

62. Pessoa L. On the relationship between emotion and cognition. *Nat Rev Neurosci*. 2008;9:148–158. doi: 10.1038/nrn2317
63. Hart SJ, Green SR, Casp M, Belger A. Emotional priming effects during Stroop task performance. *NeuroImage*. 2010;49:2662–2670. doi: 10.1016/j.neuroimage.2009.10.076
64. Sentis AI, Rasero J, Gianaros PJ, Verstynen TD. Integrating multiple brain imaging modalities does not boost prediction of subclinical atherosclerosis in midlife adults. *NeuroImage Clin*. 2022;35:103134. doi: 10.1016/j.nicl.2022.103134
65. Marek S, Tervo-Clemmens B, Calabro FJ, Montez DF, Kay BP, Hatoum AS, Donohue MR, Foran W, Miller RL, Hendrickson TJ, et al. Reproducible brain-wide association studies require thousands of individuals. *Nature*. 2022;603:654–660. doi: 10.1038/s41586-022-04492-9
66. Schönbrodt FD, Perugini M. At what sample size do correlations stabilize? *J Res Pers*. 2013;47:609–612. doi: 10.1016/j.jrp.2013.05.009
67. Elliott ML, Knodt AR, Ireland D, Morris ML, Poulton R, Ramrakha S, Sison ML, Moffitt TE, Caspi A, Hariri AR. What is the test–retest reliability of common task-functional MRI measures? New empirical evidence and a meta-analysis. *Psychol Sci*. 2020;31:792–806. doi: 10.1177/0956797620916786
68. Kragel PA, Han X, Kraynak TE, Gianaros PJ, Wager TD. Functional MRI can be highly reliable, but it depends on what you measure: a commentary on Elliott et al. (2020). *Psychol Sci*. 2021;32:622–626. doi: 10.1177/0956797621989730
69. Lovallo WR, Gerin W. Psychophysiological reactivity: mechanisms and pathways to cardiovascular disease. *Psychosom Med*. 2003;65:36–45. doi: 10.1097/01.PSY.0000033128.44101.C1
70. Barnett PA, Spence JD, Manuck SB, Jennings JR. Psychological stress and the progression of carotid artery disease. *J Hypertens*. 1997;15:49–55. doi: 10.1097/00004872-199715010-00004
71. James LR, Brett JM. Mediators, moderators, and tests for mediation. *J Appl Psychol*. 1984;69:307–321. doi: 10.1037/0021-9010.69.2.307
72. Judd CM, Kenny DA. Process analysis: estimating mediation in treatment evaluations. *Eval Rev*. 1981;5:602–619. doi: 10.1177/0193841X8100500502
73. Kenny DA, Judd CM. Power anomalies in testing mediation. *Psychol Sci*. 2014;25:334–339. doi: 10.1177/0956797613502676
74. O'Rourke HP, MacKinnon DP. When the test of mediation is more powerful than the test of the total effect. *Behav Res Methods*. 2015;47:424–442. doi: 10.3758/s13428-014-0481-z
75. O'Rourke HP, MacKinnon DP. Reasons for testing mediation in the absence of an intervention effect: a research imperative in prevention and intervention research. *J Stud Alcohol Drugs*. 2018;79:171–181. doi: 10.15288/jsad.2018.79.171
76. Kleckner IR, Zhang J, Touroutoglou A, Chanes L, Xia C, Simmons WK, Quigley KS, Dickerson BC, Feldman BL. Evidence for a large-scale brain system supporting allostasis and interoception in humans. *Nat Hum Behav*. 2017;1:0069. doi: 10.1038/s41562-017-0069
77. Zhang J, Chen D, Srirangarajan T, Theriault J, Kragel PA, Hartley L, Lee KM, McVeigh K, Wager TD, Wald LL, et al. Cortical and subcortical mapping of the allostatic-interoceptive system in the human brain: replication and extension with 7 Tesla fMRI. *BiorXiv*. 2023. doi: 10.1101/2023.07.20.548178
78. Baas D, Aleman A, Kahn RS. Lateralization of amygdala activation: a systematic review of functional neuroimaging studies. *Brain Res Rev*. 2004;45:96–103. doi: 10.1016/j.brainresrev.2004.02.004
79. Dar T, Radfar A, Abohashem S, Pitman RK, Tawakol A, Osborne MT. Psychosocial stress and cardiovascular disease. *Curr Treat Options Cardiovasc Med*. 2019;21:23. doi: 10.1007/s11936-019-0724-5
80. Vaccarino V, Bremner JD. Stress and cardiovascular disease: an update. *Nat Rev Cardiol*. 2024;21:603–616. doi: 10.1038/s41569-024-01024-y
81. Gianaros PJ, Hariri AR, Sheu LK, Muldoon MF, Sutton-Tyrrell K, Manuck SB. Preclinical atherosclerosis covaries with individual differences in reactivity and functional connectivity of the amygdala. *Biol Psychiatry*. 2009;65:943–950. doi: 10.1016/j.biopsych.2008.10.007
82. Gianaros PJ, Sheu LK, Remo AM, Christie IC, Crtichley HD, Wang J. Heightened resting neural activity predicts exaggerated stressor-evoked blood pressure reactivity. *Hypertension*. 2009;53:819–825. doi: 10.1161/HYPERTENSIONAHA.108.126227
83. Ryan JP, Sheu LK, Gianaros PJ. Resting state functional connectivity within the cingulate cortex jointly predicts agreeableness and stressor-evoked cardiovascular reactivity. *NeuroImage*. 2011;55:363–370. doi: 10.1016/j.neuroimage.2010.11.064
84. Tawakol A, Ishai A, Takx RA, Figueroa AL, Ali A, Kaiser Y, Truong QA, Solomon CJ, Calcagno C, Mani V, et al. Relation between resting amygdalar activity and cardiovascular events: a longitudinal and cohort study. *Lancet*. 2017;389:834–845. doi: 10.1016/S0140-6736(16)31714-7
85. Preacher KJ, Kelley K. Effect size measures for mediation models: quantitative strategies for communicating indirect effects. *Psychol Methods*. 2011;16:93–115. doi: 10.1037/a0022658
86. Lachowicz MJ, Preacher KJ, Kelley K. A novel measure of effect size for mediation analysis. *Psychol Methods*. 2018;23:244–261. doi: 10.1037/met0000165
87. Lloyd-Jones DM, Allen NB, Anderson CAM, Black T, Brewer LC, Foraker RE, Grandner MA, Lavretsky H, Perak AM, Sharma G, et al. Life's essential 8: updating and enhancing the American Heart Association's construct of cardiovascular health: a presidential advisory from the American Heart Association. *Circulation*. 2022;146:e18–e43. doi: 10.1161/CIR.0000000000001078
88. Spencer C, Reed RG, Votruba-Drzal E, Gianaros PJ. Psychological stress and the longitudinal progression of subclinical atherosclerosis. *Health Psychol*. 2024;43:58–66. doi: 10.1037/hea0001333
89. Jennings JR, Heim AF, Kuan DC-H, Gianaros PJ, Muldoon MF, Manuck SB. Use of total cerebral blood flow as an imaging biomarker of known cardiovascular risks. *Stroke*. 2013;44:2480–2485. doi: 10.1161/STROKEAHA.113.001716
90. Sojkova J, Najjar SS, Beason-Held LL, Metter EJ, Davatzikos C, Kraut MA, Zonderman AB, Resnick SM. Intima-media thickness and regional cerebral blood flow in older adults. *Stroke*. 2010;41:273–279. doi: 10.1161/STROKEAHA.109.566810
91. Abdulrahman H, van Dalen JW, den Brok M, Latimer CS, Larson EB, Richard E. Hypertension and Alzheimer's disease pathology at autopsy: a systematic review. *Alzheimers Dement*. 2022;18:2308–2326. doi: 10.1002/alz.12707
92. Ou Y-N, Tan C-C, Shen X-N, Xu W, Hou X-H, Dong Q, Tan L, Yu J-T. Blood pressure and risks of cognitive impairment and dementia: a systematic review and meta-analysis of 209 prospective studies. *Hypertension*. 2020;76:217–225. doi: 10.1161/HYPERTENSIONAHA.120.14993
93. Cox SR, Lyall DM, Ritchie SJ, Bastin ME, Harris MA, Buchanan CR, Fawns-Ritchie C, Barbu MC, de Nooij L, Reus LM, et al. Associations between vascular risk factors and brain MRI indices in UK Biobank. *Eur Heart J*. 2019;40:2290–2300. doi: 10.1093/eurheartj/ehz100
94. Alvarez-Bueno C, Cunha PG, Martinez-Vizcaino V, Pozuelo-Carrascosa DP, Visier-Alfonso ME, Jimenez-Lopez E, Cavero-Redondo I. Arterial stiffness and cognition among adults: a systematic review and meta-analysis of observational and longitudinal studies. *J Am Heart Assoc*. 2020;9:e014621. doi: 10.1161/JAHA.119.014621
95. Hughes TM, Wagenknecht LE, Craft S, Mintz A, Heiss G, Palta P, Wong D, Zhou Y, Knopman D, Mosley TH, et al. Arterial stiffness and dementia pathology: Atherosclerosis Risk in Communities (ARIC)-PET Study. *Neurology*. 2018;90:e1248–e1256. doi: 10.1212/WNL.0000000000005259
96. Scheinost D, Noble S, Horien C, Greene AS, Lake EMR, Salehi M, Gao S, Shen X, O'Connor D, Barron DS, et al. Ten simple rules for predictive modeling of individual differences in neuroimaging. *NeuroImage*. 2019;193:35–45. doi: 10.1016/j.neuroimage.2019.02.057
97. Kohoutová L, Heo J, Cha S, Lee S, Moon T, Wager TD, Woo C-W. Toward a unified framework for interpreting machine-learning models in neuroimaging. *Nat Protoc*. 2020;15:1399–1435. doi: 10.1038/s41596-019-0289-5